James Webb Space Telescope Wavefront Sensing and Control Algorithms

D. S. Acton[1], P. Atcheson[1], M. Cermak[1], L. Kingsbury[1], F. Shi[2], D. C. Redding[2]

[1]Ball Aerospace & Technologies Corp.
[2]Jet Propulsion Laboratory

Abstract

The Northrup-Grummann/Ball/Kodak team is building the James Webb Space Telescope (JWST), scheduled for launch in 2011. Part of Ball's responsibility is to develop the wavefront sensing and control (WFS&C) algorithms and software that will be used to provide the level of imaging performance needed to support the mission's science objectives.

Wavefront sensing on JWST differs from that performed on many ground-based telescopes in that it is conducted entirely within the focal plane of it's chief science camera, the Near Infrared Camera (NIRCam). In a sense, the complexity of a conventional wavefront sensor is eliminated, in favor of rather complex image processing performed on the ground, to extract the wavefront information.

This paper will describe the algorithms being developed for JWST. Specifically, we will describe algorithms for the coarse alignment of the primary mirror segments and the secondary mirror, the coarse phasing of the primary mirror segments, and the fine phasing of the entire telescope. We will also present algorithms for monitoring the wavefront quality throughout the JWST mission.

Key words – JWST, testbeds, wavefront sensing and control

1. Introduction

The James Webb Space Telescope (JWST) is a 6.5 meter, 18-segment, deployable, light-weighted, high authority, cryogenic telescope. The telescope folds up to fit into the launch vehicle, and is "unfolded" some time after launch. The Primary Mirror (PM) segments and the Secondary Mirror (SM) are controlled by 6 actuators (hexapods) which allow for 5 unique rigid body motions per element. In addition, the PM segments each have a 7^{th} actuator for adjusting the local radius of curvature, for a total of 113 unique degrees of adjustment.

When the telescope has sufficiently cooled, wavefront sensing and control (WFS&C) algorithms will be applied to image data taken with the Near Infrared Camera (NIRCam) in order to estimate the telescope wavefront errors and to determine the appropriate actuator commands needed to correct these errors. In the commissioning of the telescope, a variety of activities will be conducted in order to sense and correct the relatively large PM and SM errors associated with the telescope deployment. After the initial commissioning of the telescope is completed, Wavefront Sensing and Control (WFS&C) activities will be conducted on an as-needed basis, operating on much smaller wavefront errors. As an overriding principle, we will never make an adjustment to the primary and secondary mirrors that degrades the wavefront beyond that of the current aberrations.

The WFS&C commissioning process can be divided into 5 steps (the maintenance step is added here for clarity):

- First light and telescope focus
- Segment identification and search
- Coarse alignment
- Coarse phasing
- Fine phasing
- Wavefront monitoring and phase maintenance

Optical, Infrared, and Millimeter Space Telescopes, edited by John C. Mather,
Proceedings of SPIE Vol. 5487 (SPIE, Bellingham, WA, 2004)
0277-786X/04/$15 · doi: 10.1117/12.551846

2. First Light

The first operation in the commissioning process will be to verify that we have acquired the target star and to roughly check the telescope focus. Figure 1 (left) shows what we might see on the NIRCam detector with the SM off by 3 mm in despace (focus), and with the SM at its nominal focus position (right). The SM needs to be close to its nominal focus position in order to proceed with the segment ID stage of the commissioning process. If the focus of the telescope looks questionable at first light, we will take several images with different SM despace values. Encircled energy considerations will easily reveal the optimal position of the SM to minimize the segment focus error.

If a segment has a very large piston relative to the other segments error (e.g., a few mm), it's corresponding spot will appear defocused. If this occurs, the piston terms of the offending segments will be adjusted as necessary to roughly correct the error.

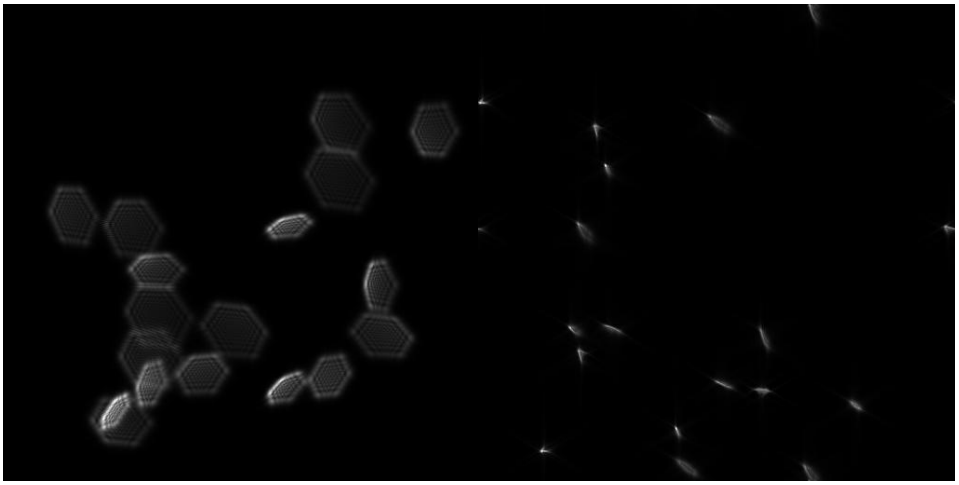

Figure 1. Example of first light image with 3 mm SM despace error (left) and at the nominal focus position (right). The SM needs to be close to the nominal focus position in order to proceed to the segment ID stage of the commissioning process.

3. Segment Identification and search

In the segment ID stage we match up the spots on the detector with their associated segments. The algorithm to identify the segments is quite simple: an initial image is taken, and the first PM segment is tilted about 5 arcseconds. A second image is taken, and the second PM segment is also tilted. This continues until 19 images are obtained and all 18 segments have been tilted by a small amount. Differences between successive images are taken, to form 18 difference maps. The unperturbed segment spots will vanish under the subtraction; the moved segment will appear as a positive/negative pair of points within the image, identifying the segment. This is illustrated in Figure 2.

The centroids of the spot pair in the difference images will help calibrate the segment tilt process, so that more accurate moves may be made during later steps of the commissioning process.

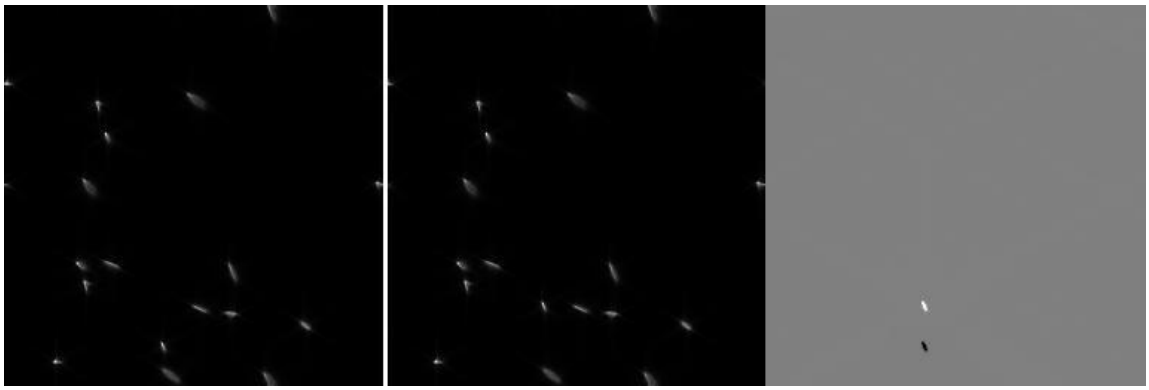

Figure 2. Images before (left) and after (middle) tilting a segment by about 5 arcseconds. Taking the difference between the two images (right) gives a clear indication of the spot associated with the tilted segment.

In all likelihood, each of the 18 PM segment spots will fall within the NIRCam science field. However, there is a reasonable chance that one or more of the segments will not be found. In this case, a spiral search pattern will instigated, taking images in between moves, until the missing segments are found.

At the completion of the segment identification process, the location of each segment spot will be known, as well as a reasonable calibration of the segment tip/tilt gains. The segments will be tilted as necessary so as to put the spots in a hexagonal array to match that of the primary mirror geometry. The center of the hexagonal array will be coincident with the mean centroid location of all the segments. The moves will be accomplished in two or more steps—pausing to record images in between steps—to make an even better determination of the segment tip/tilt gains. When the spots are finally arranged in a hexagonal pattern, we will be ready to begin the next step in the commissioning process.

4. Coarse Alignment

The purpose of the coarse alignment stage is to place the secondary mirror in the right location, and to reduce rigid body errors in the individual PM segments so that the overall segment level wavefront is less than about 200 nm rms, not counting tip, tilt, or piston errors. 3 or more images are taken with different amounts of defocus, as shown in Fig. 3. The defocus is introduced by changing the despace of the SM. Note that changing the secondary despace also changes the relative spacing between the segment spots.

The basic flow of the coarse alignment algorithm is shown in Fig. 4. Each image is parsed up into 18 sub-images, so that the Modified Gerchberg Saxton (MGS) algorithm (described in Section 8) can be applied to the segments individually, yielding the wavefront errors on a segment level. The retrieved phase maps from each segment are decomposed into "Hexikes:" a version of Zernike Polynomials defined on a hexagon rather than a unit circle [1]. The Hexike coefficients uniquely determine the 5 alignment terms for the SM: X-tilt, Y-tilt, X-decenter, Y-decenter, despace (focus). Large rigid-body motions of the PM segments will also be corrected in the coarse alignment stage.

Note that there is no ambiguity between the SM tilt and decenter terms: this is because the SM has a large aspheric departure. It is important to point out, however, that ambiguity can occur between PM modes and SM misalignments. When the PM is deployed, the segments will experience random rigid-body misalignments. Taken as a whole, the net PM wavefront may contain modes that are indistinguishable from those associated with rigid-body motions of the SM. Those PM modes will end up being corrected by moving the SM, resulting in a slight misalignment between the PM and the SM. Although the wavefront at a single point on NIRCam will still end up being quite acceptable, the PM/SM misalignment may create unacceptable aberrations at other points within the JWST science field.

The magnitude of the effect of PM/SM misalignment is currently being analyzed. One obvious solution to this problem is to measure the wavefront at more than one point within NIRCam, or perhaps even on JWST's other science instruments. Taken together, a unique solution can be found for both the PM and the SM that gives good performance across the entire JWST science field.

The final activity in coarse alignment is to move the segment spots so that they fall on top of each other. This operation, known as "image stacking" is difficult to do without knowing the exact tip and tilt gains of each segment. Consequently, image stacking will be performed in several steps, making intermediate measurements of the spot centroids and adjustments to the segment control laws.

As an alternative to the above multi-step stacking process, we are also considering a different approach known as "Large Dynamic Range Tilt Retrieval." This technique, developed by JPL, makes a single attempt to stack the images, and then relies on the MGS algorithm to determine the residual segment tilts, even though large piston errors between the segments may remain. This approach offers much promise and may be used as a supplement or backup to the multi-step stacking process.

After completion of the coarse alignment process, all wavefront errors (except PM segment piston) should be less than 200 nm rms.

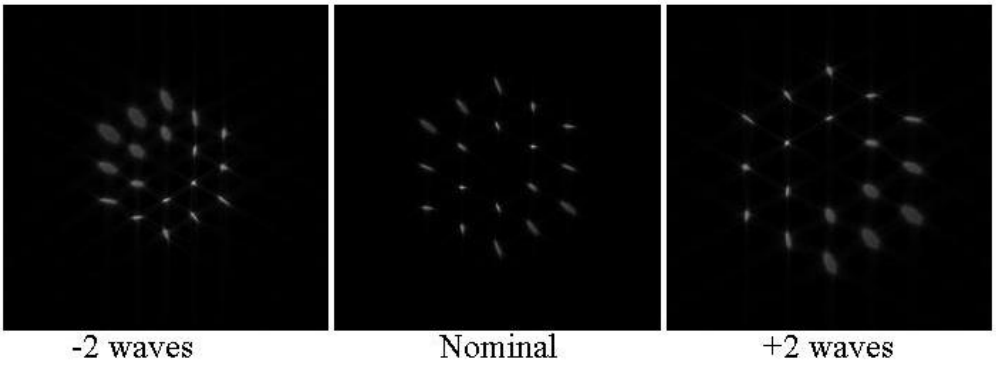

Figure 3. Segment images arranged in a hexagonal pattern for coarse alignment. Defocus is introduced by changing the despace term of the SM.

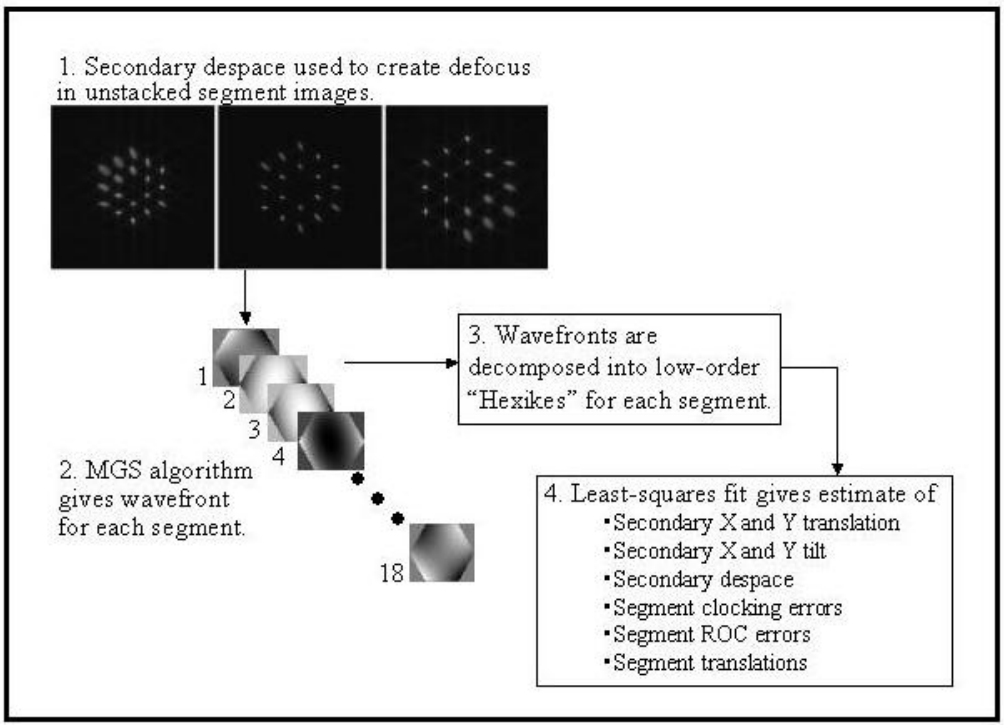

Figure 4. The basic Coarse Alignment process.

5. Coarse Phasing

Very large PM segment piston errors should have been removed during the First Light stage. However, somewhat smaller errors (~100 microns PTV) may remain. The purpose of the Coarse Phasing process is to sense these errors and correct them to about 200 nm rms.

The Coarse Phasing operations will be based on Dispersive Fringe Sensing (DFS) techniques. A dispersive element (a diffraction grating plus a prism) is placed at an image of the JWST PM within NIRCam. A pair of segments will produce a characteristic image that resembles a "barber-pole" as shown in Fig. 5. The angle and spacing of the fringes uniquely determines the pistons error between the pair of segments.

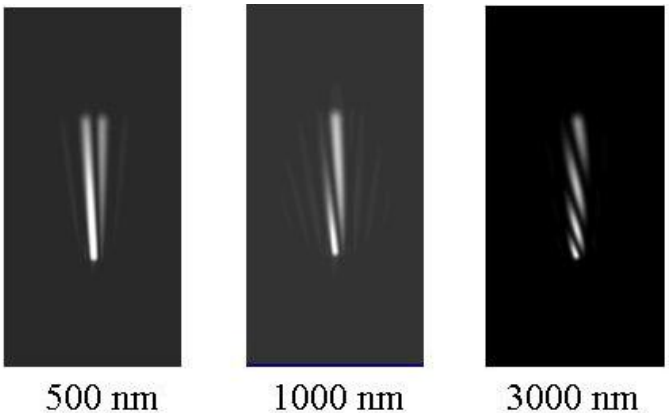

Figure 5. Dispersed fringes indicating a piston error between 2 segments.

Our baseline Coarse Phasing approach uses a novel design for dispersive element that allows the relative piston value of each segment to be determined with only two separate measurements. We will place dispersive elements into the filter wheel of NIRCam, which is located at an image of the PM. The dispersive elements yield the relative piston term between pairs of segments. By making many such measurements simultaneously, it is possible to solve for the relative piston values of all 18 segments. Because of its use of multiple subapertures, we refer to this approach as a "Dispersed Hartmann Sensor" (DHS). Algorithms to analyze the fringe patterns and to solve for the piston errors are being developed by Adaptive Optics Associates.

Another approach is being developed by JPL [4] for phasing the PM segments. This approach follows a more conventional application of a DFS. Two dispersive elements are placed in the NIRCam filter wheels. The dispersive elements have a diffraction grating and a single wedge. The gratings are orientated 90 degrees with respect to each other. (Note that these elements lack the complex masking used in the DHS approach.)

Piston is sensed and corrected in a multi-step process, which is illustrated in Fig. 6. (Note that the pupil geometry has been rotated 30 degrees for clarity.) In Fig. 6, the darkly shaded segments represent those that are currently phased with respect to the reference. The lightly shaded segments are those that are being examined and phased in the current step. The white segments are tilted off to the side so as to not confuse the phase of the active segments.

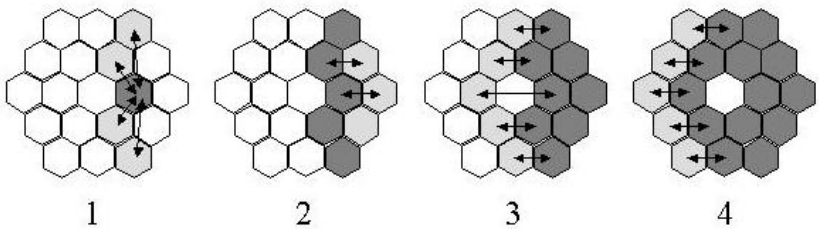

Figure 6. Four steps of the DFS process. In the first step, the 4 lightly-shaded segments are adjusted in piston to be in phase with the center darkly-shaded segment. In steps 2-4, the lightly shaded segments are adjusted to be in phase with the corresponding phased segment(s) in each row.

In the first step, a vertical "column" of segments is phased so that each of the segments in this column can be used a reference segment in the subsequent steps. The segments are adjusted in piston to be phased with respect to the reference segment, one at a time. After all 4 segments are phased against the reference segment, a small amount of vertical tilt is placed in these segments so that the spots do not interfere with each other. This creates 5 reference segments for phasing the rows of segments in subsequent steps.

In the second step, the 3 lightly shaded segments are adjusted in piston until they are matched with their neighboring reference segments. Note that all three piston terms can be measured at the same time, since the 3 fringe patterns do not fall on top of each other, owing to the small vertical tilt placed in the reference segments.

In steps 3 and 4, the remaining segments are phased up with their corresponding reference segments. When all piston errors are corrected, each row of segments is tilted back to be coincident with the original reference segment.

After application of either the DHS or DFS process, the wavefront should be fully corrected except for small errors that remain from the Coarse Alignment process, and any new errors that are created when making large piston adjustments. These errors will be measured and removed in the Fine Phasing process.

6. Fine phasing

The Fine Phasing process estimates the wavefront phase and derives the appropriate PM and SM mirror commands needed to correct the errors. Much of this process is identical to the Coarse Alignment process: the phase is estimated by applying the MGS algorithm to defocused images, and the mirror updates are generated exactly as described in Fig. 4. In this case, however, defocus is introduced to the images by inserting weak defocusing elements into the beam in NIRCam. The defocusing elements are in the filter wheel which is located at an image of the telescope pupil. The segment images are stacked on top of each other; consequently, the phase of the entire telescope is estimated from a single set of images, instead of 18 sub-sets as in the Coarse Alignment process.

The phase errors going into the Fine Phasing process are expected to be only a few hundred nm rms. An example of a simulated Fine Phase estimation is shown in Fig. 7.

7. Monitoring and maintenance

After completion of the Fine Phasing process, the wavefront errors in the telescope should be about 100 nm rms, which is adequate to achieve the JWST science objectives. Our current plan is to monitor the image quality and/or wavefront frequently from the science imagery, and make routine applications of the Fine Phasing process using a pre-selected target star.

If a science image contains a well-exposed unresolved star, it is possible to determine the Strehl ratio of the image (measured peak of the PFS divided by it's theoretical diffraction-limited value) and infer the rms wavefront errors using the Marechal approximation of the Strehl Ratio:

$$S = e^{-(2\pi\sigma)^2}$$

σ is the rms phase error, in waves. An rms wavefront error of 150 nm would produce a Strehl Ratio of 0.8 at a wavelength of 2 microns, which should be observable in a well-exposed stellar image.

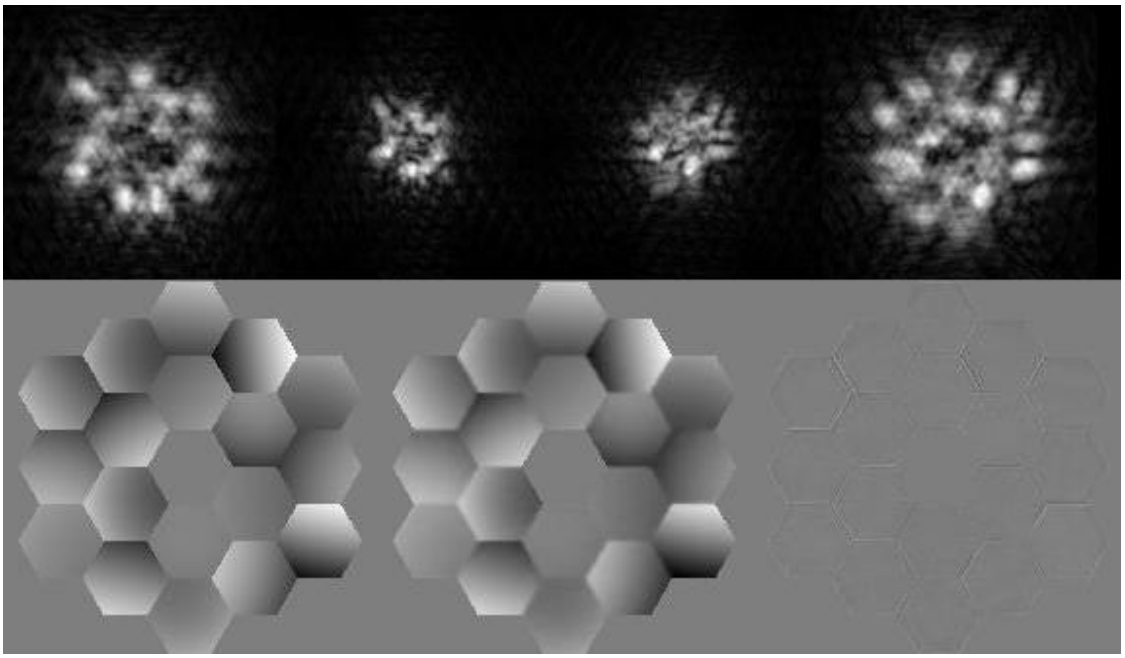

Figure 7. Fine phasing example. Top: simulated images with defocus values of –6, -3, 3, 6 waves PTV (log display). Lower left: the actual phase map (~250 nm rms). Lower center: estimated phase. Lower right: difference (~10 nm rms).

We also have the option of taking defocused images using the current science field, and applying the Fine Phasing algorithm. For this purpose, we would use only 2 defocused images—or perhaps even a single image—defocused by 2 waves PTV. It can be shown that using 1 or 2 weakly defocused images instead of 4 highly defocused images, only results in a modest decrease in accuracy in the phase estimation process, provided the wavefront errors are not large. (This will certainly be the case during science observations.)

A magnitude 16 star is sufficient to obtain the defocused images with integration times of ~1 minute. Stellar density curves predict that a magnitude 16 star should be available somewhere in the NIRCam science field of view about 70% of the time. Consequently, wavefront measurements could be made without having to slew the telescope to a pre-selected WFS&C star, and would take away less than 5 minutes of science time. Therefore, this presents us with a very important contingency for maintaining a good wavefront on the telescope if the alignment were to drift faster than the currently hoped (~ 30 days).

8. Modified Gerchberg-Saxton Algorithm

The classic Gerchberg-Saxton algorithm estimates the wavefront phase from a single focused image [2]. The algorithm is actually very simple: the complex pupil function is transformed back and forth from the image plane to the pupil plane through the use of Fast Fourier Transforms (FFT's), applying the known amplitude constraints at each step. In the image plane, the amplitude is simply the square-root of the recorded image. In the pupil plane, the amplitude is just the geometry of the aperture. After many iterations, the phase obtained in the pupil plane converges to the desired wavefront.

A block diagram of the classic Gerchberg-Saxton algorithm is shown in Fig. 8. The actual heart of the algorithm is shown in the dotted box. The rest of the flow exists to handle low-order phase terms (such as the known defocus value) that might otherwise create wrapping in the phase term. The low-order terms are "offloaded" to separate arrays and passed in and out of the pupil function through the use of complex phase kernels.

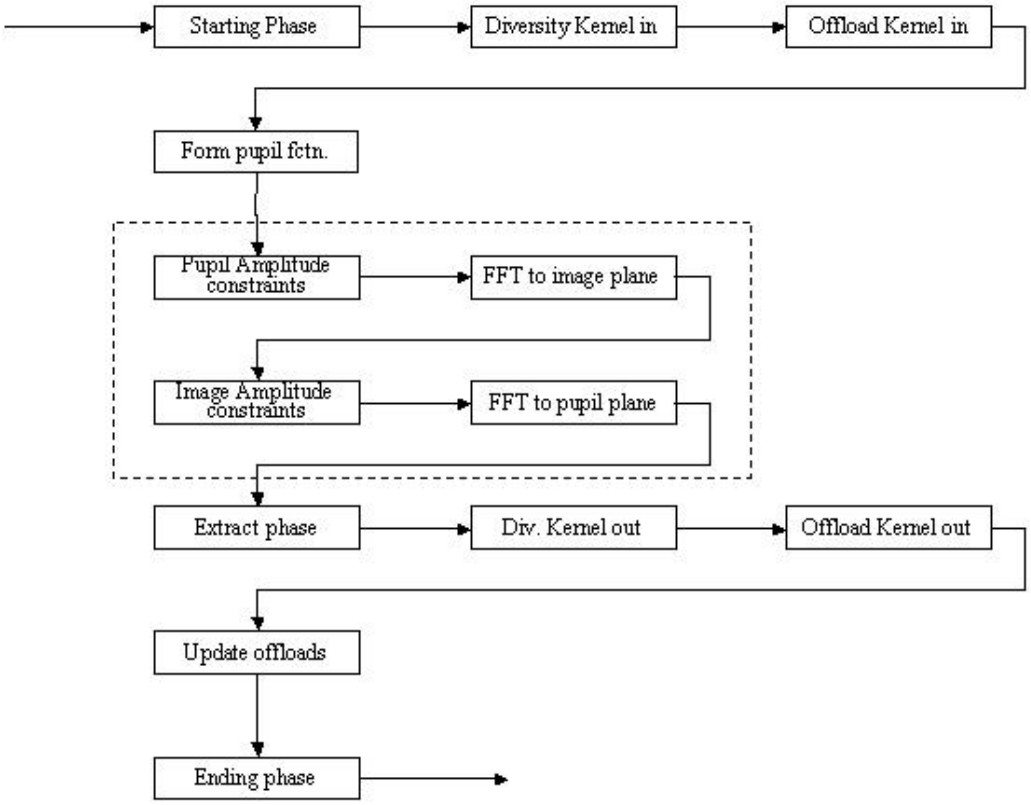

Figure 8. The classic Gerchberg-Saxton algorithm.

The Modified Gerchberg-Saxton (MGS) algorithm makes use of several images, that are biased by a known defocus term. The classic Gerchberg-Saxton algorithm is applied to each image, producing an estimate of the pupil phase. A weighted average of the phases is formed, and used as a starting estimate of the phase for the application of the classic Gerchberg-Saxton algorithm on the individual images. The process is repeated several times, resulting in a very accurate estimate of the nominal wavefront.

A block diagram of the MGS algorithm is shown in Fig. 9. The images are pre-processed to reduce noise and interpolated to the desired plate scale. They are also shifted so that their centroids are registered with respect to each other. We have found that the image registration needs to be done very precisely. Registration based on the image centroid only achieves this in an approximate sense; the true registration must be done by reconstructing the phase and shifting each image so that the mean tilt in the wavefront is zero. Consequently, about ½ of the MGS process is spent just registering the images. Occasionally, the final wavefront estimate is taken, yet again, to aid in the registration of the images, repeating the entire process.

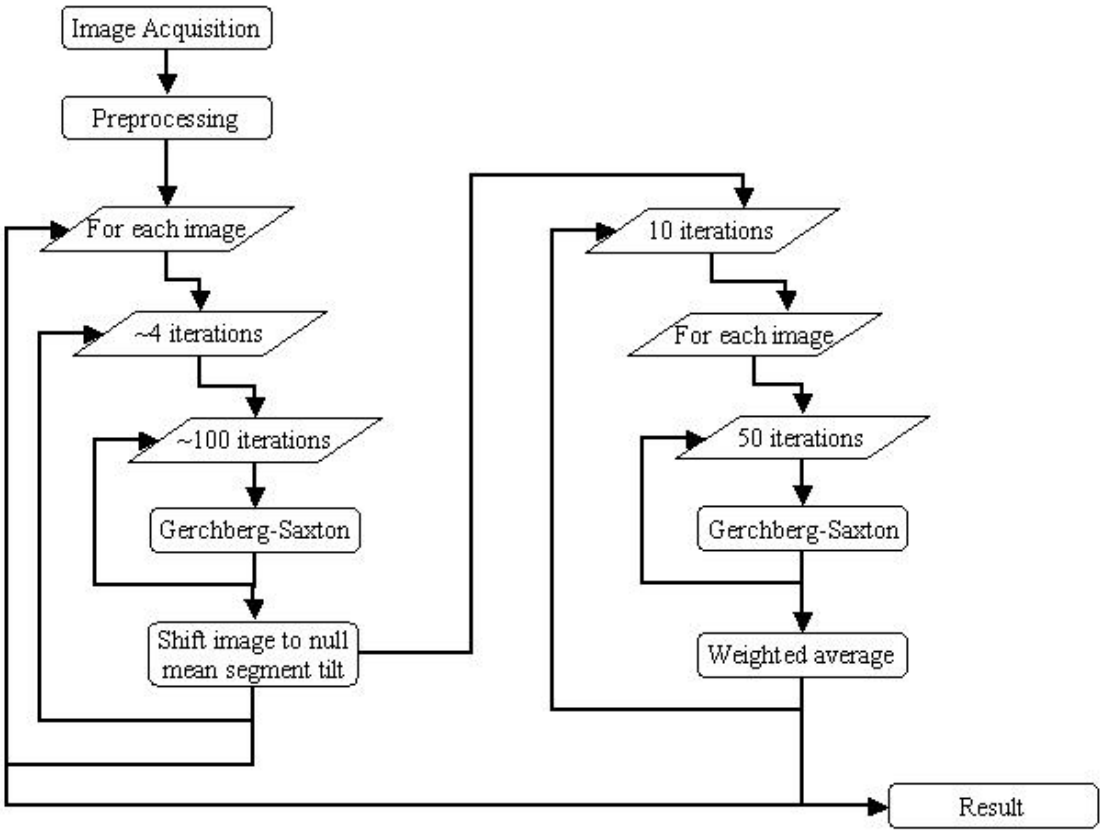

Figure 9. The Modified Gerchberg-Saxton algorithm.

9. Lab Experiments

A scale model of JWST is currently being constructed by Ball Aerospace for testing and developing WFS&C algorithms [3]. We have also performed extensive testing and development using the High Authority Primary Mirror (HAPM) optical test facility at Ball Aerospace. This facility uses a 3 mirror telescope with a 6-segment primary mirror. Each segment has 4 degrees of freedom: tip, tilt, piston and radius of curvature adjustment. The secondary mirror in the telescope has 5 degrees of freedom. A picture of the primary mirror is shown in Fig. 10

All of the algorithms except for the Coarse Phasing process have been demonstrated on the HAPM test facility. A sample of the phase retrieval results obtained in shown in Fig. 11. The errors detected were created by misaligning the pupil image on a spherical aberration corrector in the telescope.

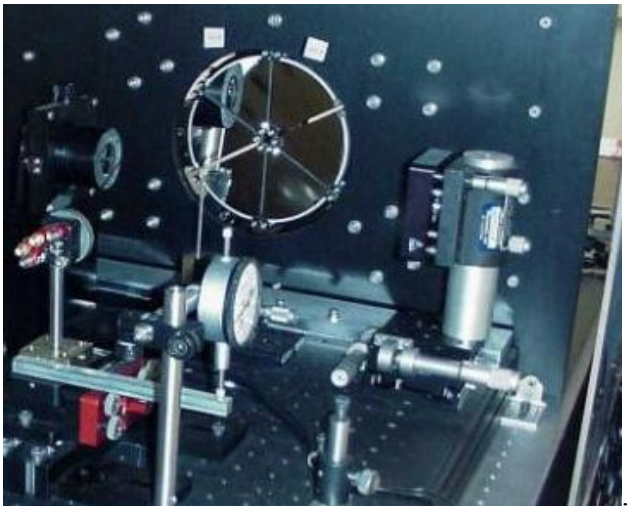

Figure 10. The High Authority Primary Mirror (HAPM).

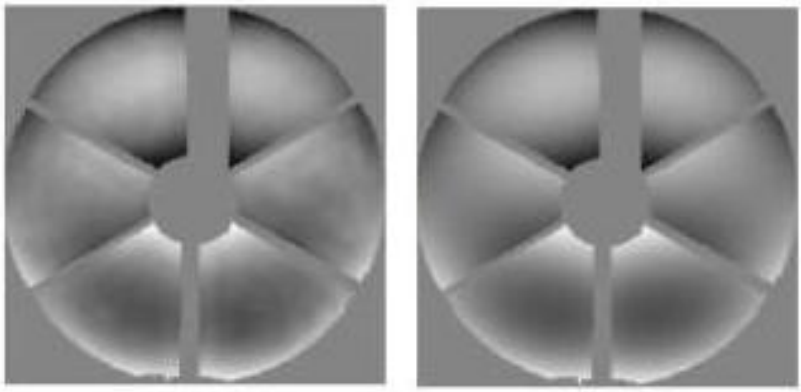

Figure 11. Experimental phase retrieval results (left) and theoretical prediction (right).

10. Acknowledgements

The authors would like to gratefully acknowledge the enormous contributions to the JWST WFS&C algorithm development effort by JPL, GSFC, and General Dynamics.

11. References

1. C. F. Dunkl, "Orthogonal Polynomials on the Hexagon." SIAM J. Appl. Math. 47(2) 1987.

2. R. W. Gerchberg and W. O. Saxton, "A practical algorithm for the determination of phase from image and diffraction plane pictures," Optik 35 (1972).

3. P. Atcheson, L. Kingsbury, D. S. Acton, "JWST Telescope Testbed for WFS&C Algorithm and Software Development," these proceedings.

4. D. C. Redding, F. Shi, S. A. Basinger, D. Cohen, J. Green, A. E. Lowman, C. M. Ohara, "Wavefront Sensing and Control for Large Space Optics," Proceedings of the Big Sky Conference, Bozeman, Montana, 2003.